Characterizing solids mixing in DEM simulations

W. Godlieb, N.G. Deen and J.A.M. Kuipers

University of Twente, Faculty of Science and Technology, Institute for Mechanics Processes and Control Twente,
P.O. Box 217, NL-7500 AE Enschede, The Netherlands and
Dutch Polymer Institute, PO Box 902, 5600 AX Eindhoven, The Netherlands;
E-mail: N.G.Deen@utwente.nl

Keywords: solids mixing, fluidized bed, granular matter, DEM simulation

Abstract

In the production and processing of granular matter, solids mixing plays an important role. Granular materials such as sand, polymeric particles and fertilizers are processed in different apparatus such as fluidized beds, rotary kilns and spouted beds. In the operation of these apparatus mixing often plays an important role, as it helps to prevent formation of hot-spots, off-spec products and undesired agglomerates. DEM can be used to simulate these granular systems and provide insight in mixing phenomena. Several methods to analyse and characterize mixing on basis of DEM data have been proposed in the past, but there is no general consensus on what method to use.
In this paper we discuss various methods that are able to give quantitative information on the solids mixing state in granular systems based on DEM simulations. We apply the different methods to full 3D DEM simulations of a fluidized bed at different operating pressures.
The following analysis methods will be investigated: average height method, Lacey index, nearest neighbours method, partner distance method and the sphere radius method. It is found that some of these methods are grid dependent, are not reproducible, are sensitive to macroscopic flow patters and/or are only able to calculate overall mixing indices, rather than indices for each direction. We compare some methods described in literature and in addition propose two new methods, which do not suffer from the disadvantages mentioned above.
We applied each of these aforementioned methods to full 3D discrete particle simulations (DPM) with $280 \cdot 10^3$ particles and we performed simulations for seven different operating pressures. We found that, mixing improves with operating pressure caused by increased porosity and the increased granular temperature of the particulate phase.

Introduction

Gas fluidized beds are widely used in industry in various large-scale processes involving physical and/or chemical operations. The large surface area of the granular media in fluidized beds is beneficial for various operations, a.o. gas-solid reactions, cooling and drying. In many cases it is important that all particles are well mixed so that all particles are cooled, reacted or dried in a similar manner, to prevent hot spot or agglomerate formation.
Solids mixing of granular materials is researched widely. Since solids mixing is difficult to characterize experimentally, some groups use discrete element models (DEM) or discrete particle models (DPM) to investigate solids mixing behaviour. McCarthy et al. (2000) succeeded to validate their simulations with experiments, which indicates that modelling is a promising approach to describe solids mixing in detail.
In this work we investigate the capabilities of five different methods that can be used to calculate a *mixing index* from DPM simulations of fluidized beds. The *mixing index* (M) is used to quantify the state of mixedness of the system and is zero or one for respectively fully demixed and fully mixed conditions. The mixing index is also known as *entropy of mixing (*Schutyser et al. 2001), Lu & Hsiau (2005) call it *mixing degree* whereas, Finnie et al. (2005), Asmar et al. (2002) and Van Puyvelde (2006) call it *mixing index*. While most authors try to determine the mixing index from DEM simulations, they use different methods: Schutyser et al. (2001) calculated entropy based on entropy equations from molecular dynamics whereas Mostoufi & Chaouki (2001) used the "colour" of a marked region (a spot) in the middle of the bed and measured the radius of the spot as a function of time. They were not able to calculate a mixing index. A similar method is described in this work. We will show that this method fails if macroscopic flow patterns are dominant. Lu & Hsiau (2005) and Rhodes et al. (2001) use the Lacey index as mixing index, which will be described later.
We propose two new methods to quantify mixing: one based on the colouring of the twelve nearest neighbours and a method based on the increasing distance of initially neighbouring particles. In this work we use the three aforementioned methods and the two newly proposed methods to investigate solids mixing in a fluidized bed containing mono disperse polymeric particles at different operating pressures. In the first part of this paper the governing equations of the DPM are presented, followed by the various solids mixing characterization methods. Subsequently the results of the application of mixing methods to our DPM simulations are discussed and conclusions are presented.

Governing Equations

The discrete particle model (DPM) is an Euler-Lagrange model, which was originally developed by Hoomans et al. (1996). In the DPM every particle is individually tracked accounting for particle-particle and particle-wall collisions.

In the DPM the gas phase hydrodynamics is described by the Navier-Stokes equations:

$$\frac{\partial}{\partial t}(\varepsilon_g \rho_g) + \nabla \cdot (\varepsilon_g \rho_g \overline{u}_g) = 0$$
$$\frac{\partial}{\partial t}(\varepsilon_g \rho_g \overline{u}_g) + \nabla \cdot (\varepsilon_g \rho_g \overline{u}_g \overline{u}_g) = -\varepsilon_g \nabla \rho_g - \nabla \cdot (\varepsilon_g \overline{\overline{\tau}}_g) - \overline{S}_p + \varepsilon_g \rho_g \overline{g} \quad (1)$$

where $\overline{u}_g$ is the gas velocity and $\overline{\overline{\tau}}_g$ represents the gas phase stress tensor. The sink term $\overline{S}_p$, represents the drag force exerted on the particles:

$$\overline{S}_p = \frac{1}{V_{cell}} \int_{V_{cell}} \sum_{i=0}^{Npart} \frac{V_i \beta}{1-\varepsilon_g} \left(\overline{u}_g - \overline{v}_i\right) D\left(\overline{r} - \overline{r}_i\right) dV \quad (2)$$

The distribution function $D\left(\overline{r} - \overline{r}_i\right)$ is a discrete representation of a Dirac delta function that distributes the reaction force acting on the gas phase to the Eulerian grid via a volume-weighing technique. The inter-phase momentum transfer coefficient, β describes the drag of the gas-phase acting on the particles. The Ergun (1952) and Wen & Yu (1966) equations are commonly used to obtain expressions for β. However, we use the closure relation derived by Koch & Hill (2001) based on lattice Boltzmann simulations, since it has no discontinuities at high Reynolds numbers and gives good results as reported by Bokkers et al. (2004) and Link et al. (2005).
The motion of every individual particle *i* in the system is calculated from Newton's second law:

$$m_i \frac{d\overline{v}_i}{dt} = -V_i \nabla p + \frac{V_i \beta}{\varepsilon_s}\left(\overline{u} - \overline{v}_i\right) + m_i \overline{g} + F_i^{pp} + F_i^{pw} \quad (3)$$

where the forces on the right hand side are, respectively due to pressure, drag, gravity, particle-particle interaction and particle-wall interaction.
The contact forces are caused by collisions with other particles or confining walls. These collisions are described with a soft-sphere approach. This approach uses a linear spring/dash-pot model, wherein the velocities, positions and collision forces of the particles are calculated at every fixed time step via a first order time integration (Hoomans et al. 1996). The collision model takes restitution and friction effects into account. The associated collision coefficients were obtained experimentally via the method of Kharaz et al. (1999). They developed a sophisticated experimental method to obtain collision parameters for different impact angles. For more details on the implementation of the soft-sphere model we refer to the work of Ye et al. (2005) and van der Hoef et al. (2006).

Methods for characterizing mixing

In this work we use five different methods te obtain mixing indices from DPM data with mono disperse particles. In this section each of these methods will be discussed in detail.

Average height method

The average height method is the simplest of the investigated methods and is based on the average height of a group of coloured particles. It is widely used for measuring segregation, for example by Hoomans et al. (2000). In the case of mono disperse systems, half of the particles are given a colour, while all physical properties remain unchanged and constant throughout the set of particles. Subsequently the average position of all particles is monitored. While the mixing behaviour can in principle be investigated in all three directions, here we will only focus on mixing in the vertical direction. In the first step of the algorithm the vertical positions of all particles are sorted to determine the median height. Subsequently the lower half of the particles is coloured white, while the upper half is coloured black. For each time step the average height of the white particles can be calculated and normalised with the average height of all particles:

$$\overline{z}_{white} = \frac{\frac{1}{N_{white}} \sum_{i \in white} z_i}{\frac{1}{N_{all}} \sum_{i \in all} z_i} \quad (4)$$

where $\overline{z}_{white}$ is the normalised average vertical position of the white particles. Notice that initially $\overline{z}_{white}$ is 0.5 and when the system fully mixed it becomes 1.0. We now define the mixing index as follows:

$$M = 2 \cdot (\overline{z}_{white} - 0.5) \quad (5)$$

which means that for $M = 0$ the system is fully demixed and for $M = 1$ the bed is fully mixed.
This method can also be used to study lateral mixing. In those cases the left and right or bottom and top parts, are respectively coloured white and black.

Lacey's method

The Lacey index is based on statistical analysis and was developed by Lacey (1954). The variance S^2 for the concentration of the black particles in each cell is defined as follows:

$$S^2 = \frac{1}{N-1} \sum_{i=1}^{N} (\phi_i - \phi_m)^2 \quad (6)$$

where N is the number of cells in the bed containing particles and ϕ_i the concentration of black particles in cell *i* and ϕ_m the average concentration of black particles in the bed.
S_0^2 and S_R^2 are defined as:

$$S_0^2 = \phi_m (1 - \phi_m) \quad (7)$$

$$S_R^2 = \frac{\phi_m (1 - \phi_m)}{n} \quad (8)$$

and respectively represent the variance of the unmixed bed and fully mixed bed. *n* is the average number of particles per cell.

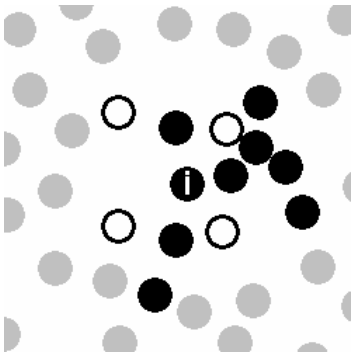

Figure 1: Illustration of the nearest neighbours method. For the highlighted particle (i) the twelve nearest neighbours are shown. Four of them are white and eight are coloured black. Particles that are located further away are coloured grey and are not taken into account for this particle.

The mixing index can be calculated as follows:

$$M = \frac{S^2 - S_0^2}{S_R^2 - S_0^2} \tag{9}$$

Due to the use of grid cells the Lacey index is grid-dependent. A coarse grid gives higher mixing indices, since in that case micro mixing effects are neglected. A fine grid gives lower mixing indices, if only few particles are present in a cell. If only one particle is present in a cell it is always fully unmixed.

Nearest neighbours method

Contrary to the average height method in which the overall average height of the particles is monitored, in the nearest neighbour method we evaluate the mixing in the vicinity of individual particles. Opposite to the Lacey index, it is grid-independent. Initially we colour half of the particles black, similar to what is done in the average height method. For each particle we determine the twelve nearest neighbouring particles. If these particles have the same colour as the particle under investigation it is unmixed, while if half of the nearest neighbours is coloured differently, it is fully mixed. This is expressed as follows:

$$M = \frac{1}{N_{part}} \sum_{N_{part}} \frac{2n_{diff}}{n_{nb}} \tag{10}$$

where n_{diff} is the number of nearest neighbours coloured differently and n_{nb} the number of nearest neighbours.
Figure 1 shows an example for one individual particle, for which four neighbouring particles have a different colour (white). The mixing index for that specific particle is 2·4/12 = 0.67. The overall mixing index is the average over all particles.

Neighbour distance method

The third method used in this work is based on the distance between initial neighbours. At a given time the nearest neighbours is located for each particle. Each particle and its nearest neighbour form a pair, and its centre to centre distance

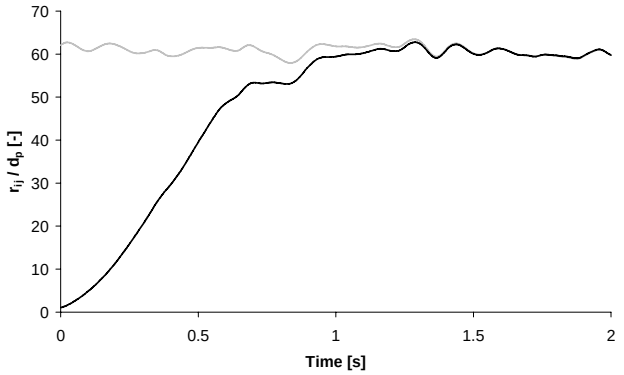

Figure 2: Distance between initial nearest neighbours averaged over all pairs (black line) and average distance between random particles (grey line).

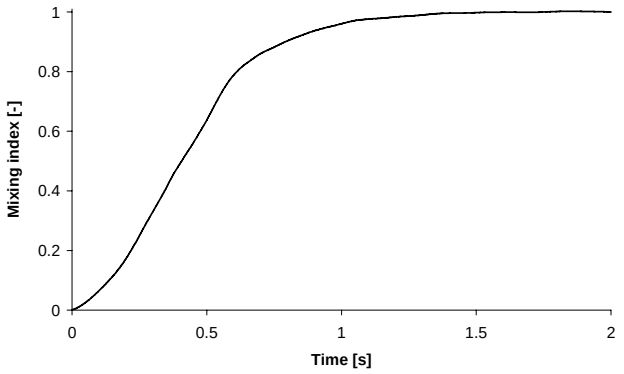

Figure 3: Mixing index determined with the neighbour distance method, calculated with the data from Figure 2.

is monitored as time progresses. Initially the distance is in the order of one particle diameter and if the bed is fully mixed it can increase up to the bed dimensions.
Figure 2 shows the average distance between initial neighbours normalized with the particle diameter. Initially it is just above one particle diameter and after 1 second it has increased up to 60 times the particle diameter. It is not a smooth curve, because bubbles let the bed expand and collapse, causing the distance between particles to increase and decrease with time. This effect introduces noise in the mixing measurement. Therefore the distance is normalised with the distance of randomly selected particle pairs, resulting in a smooth mixing curve, unaffected by bed expansions as seen in Figure 3. Since initially the distance between neighbours is one particle diameter this is set to a mixing index of 0. The mixing index is expressed in the following equation:

$$M = \frac{\sum_{i=0}^{N_{part}} r_{ij} - d_p}{\sum_{i=0}^{N_{part}} r_{ik} - d_p} \tag{11}$$

where r_{ij} is the distance between particle i and its initially nearest neighbour j and r_{ik} is the distance between particle i and a randomly selected particle k. The method just described can be used to calculate the mixing index for each direction. In that case, the same initial partner is used.

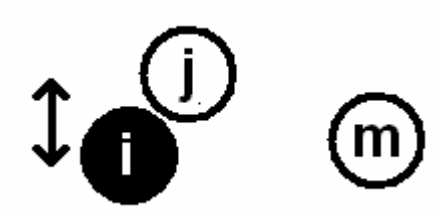

Figure 4: Mixing index determined with the neighbour distance method for the z-direction. Particle *j* is the closest partner for the highlighted particle *i*. Particle *m* has the least distance in the z-direction, but is not used as closest initial partner.

Initially the distance between the partners in one direction can be less than a diameter, as can be seen in Figure 4. Some basic algebra shows that the average distance in one direction for two touching particles is $4d_p/\pi^2$.
The mixing index in the vertical direction for the neighbour distance method is thus defined by:

$$M = \frac{\sum_{i=0}^{N_{part}} r_{ij,z} - \frac{4}{\pi^2} d_p}{\sum_{i=0}^{N_{part}} r_{ik,z} - \frac{4}{\pi^2} d_p} \tag{12}$$

The mixing index for the horizontal directions x and y can be obtained by replacing subscript z by x and y respectively.

Sphere spreading method
In their DPM simulations of a fluidized bed, Mostoufi & Chaouki (2001) coloured a box in the middle of the bed and monitored the spreading of the coloured particles. In this work we used a similar method and calculated a mixing index from the spreading of the coloured particles. Contrary to the work of Mostoufi & Chaouki (2001), we coloured a sphere, with a radius of the width of the bed, as shown in Figure 5.
The spreading of the black particles is characterised by:

$$R = \frac{1}{N_b} \sum_{i \in b} r_i \tag{13}$$

where r_i is the distance of particle *i* to the centre of mass of the set of black particles. Note that only the black particles are considered in this summation.
The mixing index can be calculated using the initial distance of the black particles R_0 and the average distance all particles R_A.

$$M = \frac{R - R_0}{R_A - R_0} \tag{14}$$

where:

$$R_A = \frac{1}{N_{part}} \sum_{i=1}^{N_{part}} r_i \tag{15}$$

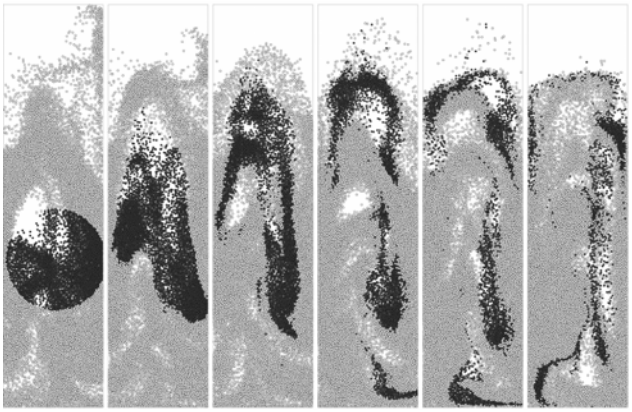

Figure 5: A slice in the middle of the fluidized bed is shown. Initially a sphere of particles is coloured black (left). After 0.2 seconds the sphere is spread over the bed (right).

Calculation of the mixing time
The mixing index is a valuable tool to investigate the solids mixing process in fluidized beds. To compare different simulations in a simple way, the mixing index curve is condensed in a single value. We choose to use the 95% mixing time $t_{95\%}$, where the mixing index reaches a value of 0.95. To prevent noise to influence the results, we fit a dampened exponential function to fit the mixing index curve as follows:

$$M_{fit} = 1 - Ae^{-\gamma t} \tag{16}$$

where A and γ, are the amplitude and the damping coefficient respectively. Each of these coefficients is obtained from the simulation data using a least squares method. The fit as shown in Figure 6 accurately follows the trend of the curve. From this fit we can calculate the mixing time at which the bed is 95% mixed, by solving eq. 16 for t:

$$t_{95\%} = \frac{-1}{\gamma} \ln\left(\frac{1 - 0.95}{A}\right) \tag{17}$$

Unfortunately the average height method and sphere spreading method show periodic overshoots. This effect is caused by the circulation patterns of the particles in the bed, as can be seen in Figure 7, which shows the mixing index obtained for the average height method. Although $M = 1$ at 0.17 seconds the bed is not fully mixed. At 0.31 seconds the

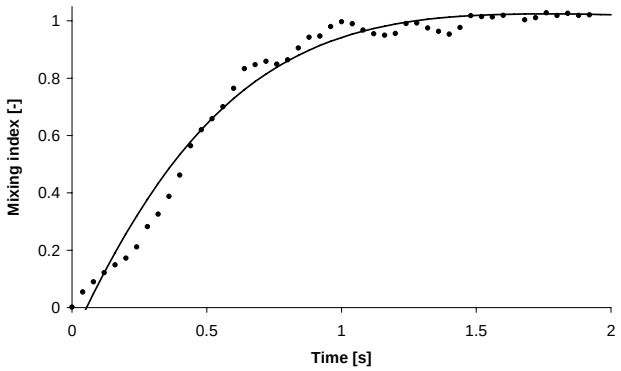

Figure 6: Lacey index fitted with a damped exponential function.

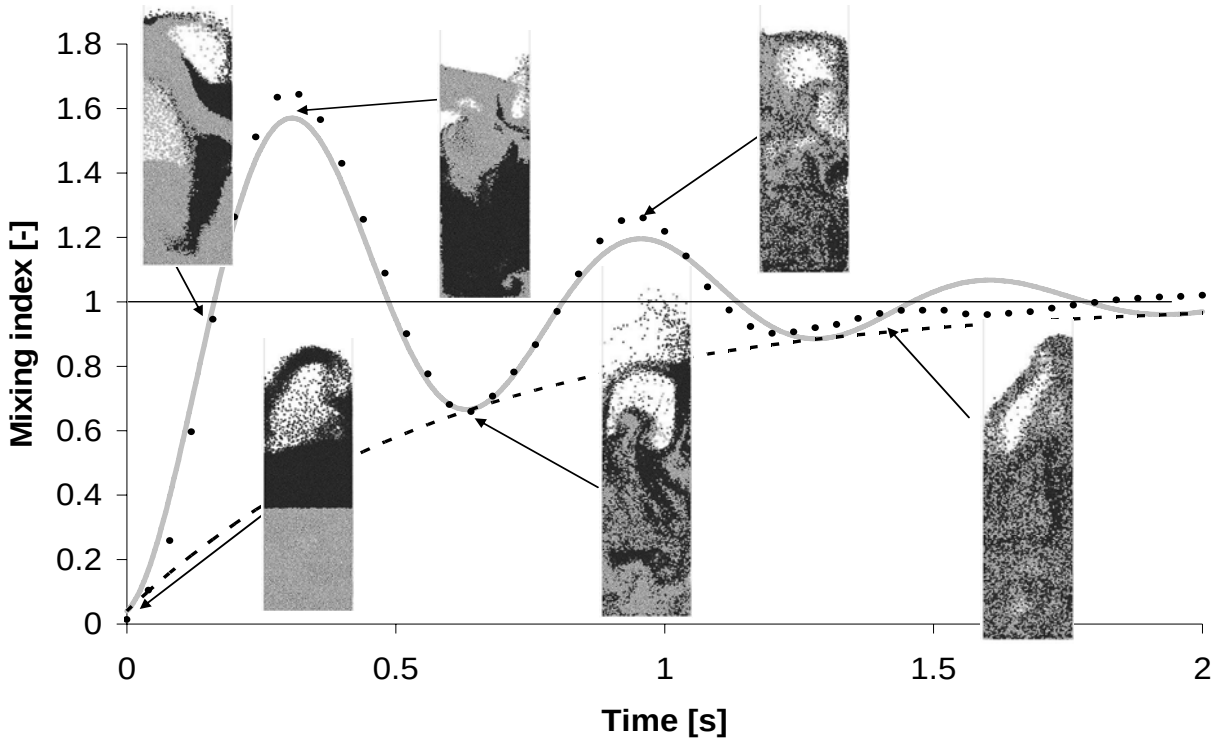

Figure 7: Mixing index versus time, resulting from simulations (•), a fit of the data using eq. 18 (—), and eq. 16 (- - -). Images of the particles present in a slice in the centre of the bed are shown as well.

colour pattern has been more or less inverted due to the bed circulation patterns, leading to an overshoot of M = 1.6. Eventually, after about 1.8 seconds the overshoots have dampened out and the bed is almost entirely mixed.
Since the mixing index is oscillating around a value of 1, it is hard to determine a mixing time; therefore the curve is fitted with a damped harmonic oscillator:

$$M_{fit} = 1 - (Ae^{-\gamma t}\cos(\omega t)) \qquad (18)$$

where ω is the period of the oscillation. Now we can calculate the 95% mixing time using the fit without the oscillator. By removing the periodic part from the fitted equation we obtain an expression similar to Eq. 6 from which a 95% mixing time can straightforwardly be obtained.

Simulation settings

To compare the performance of the different analysis methods and to investigate the pressure effect on several fluidization characteristics, seven full three dimensional DPM simulations with polymeric particles at 1, 2, 4, 8, 16, 32 and 64 bar operating pressure were performed. The system properties and operating conditions are specified in Tables 1 and 2 respectively.
We used 20 x 20 x 80 computational cells. The coefficients of restitution and the friction coefficients used in the simulations were measured according to the method described by Kharaz et al. (1999). No-slip boundary conditions were used at the confining walls.
In order to enable a proper comparison between the simulations, a constant excess velocity (i.e. superficial gas velocity minus the minimum fluidisation velocity) of 0.177 m/s was applied.

Property	symbol	value	unit
system width	X	0.025	m
system depth	Y	0.025	m
system height	Z	0.1	m
time step	dt	$1.0\cdot10^{-4}$	s
total time	t	10	s
number of particles	N_{part}	$2.86\cdot10^{5}$	-
particle diameter	r_p	0.5	mm
normal spring stiffness	k_n	200	N/m
coefficient of normal restitution	e_n	0.8	-
coefficient of tangential restitution	e_t	0.6	-
particle density	ρ	925	kg/m^3
friction coefficient	μ	0.1	-

Table 1: Settings for all seven simulations.

P (bar)	u_{mf} (m/s)	u_{sup} (m/s)
1	0.088	0.265
2	0.084	0.261
4	0.077	0.253
8	0.067	0.244
16	0.056	0.233
32	0.044	0.221
64	0.033	0.210

Table 2: Superficial gas velocities for the 3D simulations.

Results

In this section we will discuss the five methods used to calculate the mixing index, anisotropicity of the system and the influence of operating pressure on the mixing process.

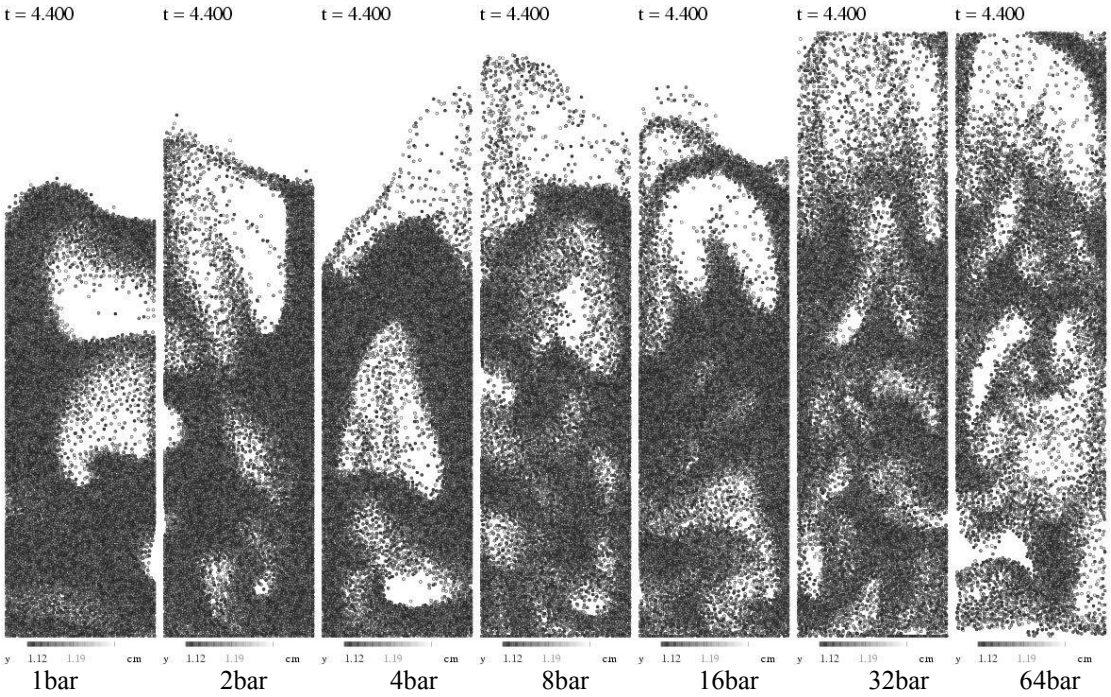

Figure 8: Snapshots of particle positions in a slice in the centre of the bed with a depth of one numerical grid cell at different operating pressures.

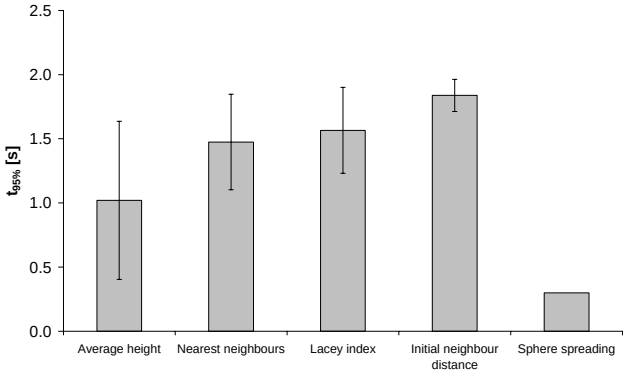

Figure 9: The 95% mixing time for all five methods for the simulation at 1 bar operating pressure. (Initially the top half of the particles were coloured black). The shown error margins are twice the standard deviation in the eight individual calculations of the 95% mixing time.

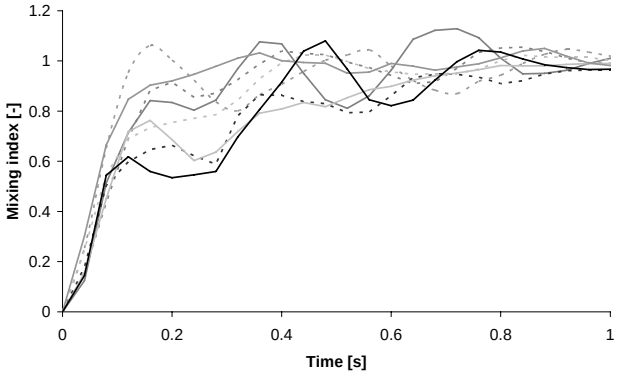

Figure 10: The mixing index calculated with the sphere radius method for 8 parts of the simulation at an operational pressure of 8 bar.

The five different mixing methods give different results for the $t_{95\%}$, due to differences in the definitions of a mixed system. We find that the sphere spreading method is less suited for the description of mixing in fluidized beds. The main reason is that it presumes a diffusive type of mixing behaviour, whereas the transport of particles in a fluidized bed is predominantly of a convective nature. As a result, the mixing index signal shows strong periodicity as the particles are circulated through the bed, as can be seen in Figure 10. The resulting signal cannot be described by a simple fit, which makes it impossible to determine an accurate mixing time.

The average height method is simple and effective, but due to the macroscopic flow pattern the colour pattern inverts, resulting in a mixing index larger than 1, as shown in Figure 7. This disadvantage complicates the data analysis of the method. Furthermore, the method cannot be used to analyse the micro mixing effect at the scale of individual particles, as it only takes macroscopic mixing into account. As a result the calculated 95% mixing time is lower than that of the other methods.

The Lacey index and the nearest neighbour method show similar results for all simulations. Both methods have a similar approach where the colouring of the neighbouring particles is taken into account. For the Lacey index we used 25 x 25 x 100 cells, so the average number of particles per cell was about twelve, which is similar to the number of neighbours taken into account in the nearest neighbours methods. The main advantage of the nearest neighbours method is its grid-independency, although the method is dependent on the number of neighbours taken into account.

The initial neighbour method gives slightly longer mixing times, but the same trend with pressure is found as for the nearest neighbour and Lacey's method, as is shown in Figure 11. The main advantage of this method is, that no grid is

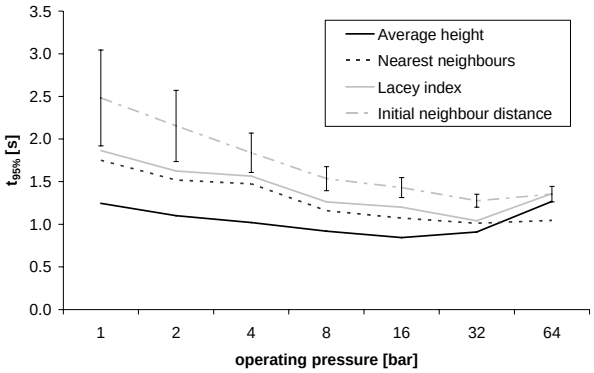

Figure 11: The 95% mixing time versus operating pressure for four different methods. For the initial neighbour distance method the error margins are shown.

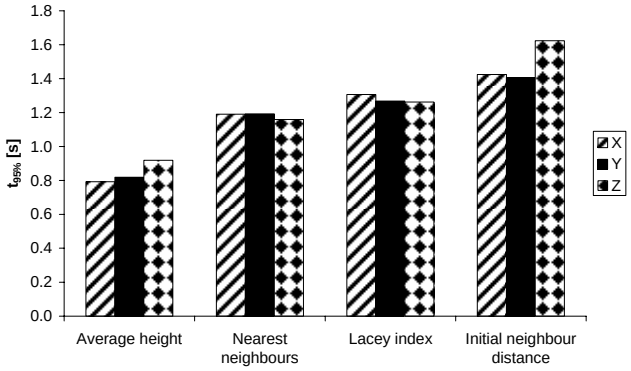

Figure 12: Mixing time for four mixing methods in vertical (z) and horizontal (x and y) directions for the simulation at 8 bar.

used in the calculation. Moreover the method is not dependent on initial colouring. All other methods discussed are based on initial colouring of particles, which influences the results. Twice the standard deviation of eight individual calculations is shown as error margins in Figure 9 and Figure 11. The error margins for this method are 12% on average which is much lower compared to the Lacey index (20%), nearest neighbours (20%) and the average height (40%) method.

Pressure influences the mixing behaviour significantly as reported earlier, see: Godlieb et al. (2006, 2007a). This is confirmed by the results shown in Figure 11. The increased number of bubbles, with more chaotic movement at elevated pressure, improves mixing. In Figure 8 it can be seen that at 64 bar the regime has changed from a bubbling regime to a more homogeneous regime. In that sense the case for 64 bar deviates from the trend in the mixing time.

Figure 12 shows the anisotropy of the mixing resulting from the four methods. The average height methods and the initial neighbour distance show a slightly larger mixing time in the vertical (z) direction, since in these methods the size of the bed is taken into account and the height of the bed is significant larger than the width and depth. We would expect anisotropic mixing, because the bubbles and gas moves in the vertical direction. However, our system appears to be too small to measure anisotropic effects.

Discussion and Conclusions

In this work we compared five different methods to calculate mixing indices from DPM simulation results (see Table 3 for a qualitative comparison). The nearest neighbour method and the initial neighbour distance method developed by the authors. Most methods are dependent on the initial colouring of the particles or the applied numerical grid. Only the method based on the distance between initial neighbours is grid and colouring independent. This method gives reproducible results with on average errors of 12%.

Besides vertical mixing, also horizontal mixing is investigated. The 95% horizontal mixing times was determined and is shown in Figure 12 along with the 95% vertical mixing time. The mixing times in all directions are of the same order, which is probably due to the limited size of the simulated system. In larger systems we would expect anisotropic mixing.

Operating pressure influences the hydrodynamics of the bed significantly: bubbles become smaller and move more chaotic, the bubble-emulsion structures becomes less distinct. Furthermore the dense phase becomes less dense at elevated pressure. Since particles have a larger degree of freedom at higher porosities it becomes easier for the particles to mix. Recently we found that the granular temperature is increased with pressure (Godlieb et al. 2007b). At high granular temperature the particles velocity has a larger fluctuating component, which enhances mixing.

Acknowledgements

This work is part of the Research Programme of the Dutch Polymer Institute (DPI) as project number #547. Contribution from the National Computing Facilities Foundation (NCF) for the use of supercomputer facilities, with financial support from the Netherlands Organisation for Scientific Research (NWO) is acknowledged.

	Reproducibility	Grid independency	Colour independency	In all directions
Average height	+	+	-	+
Nearest neighbours	+	+	-	+
Lacey index	+	-	-	+
Initial neighbour distance	++	+	+	+
Sphere radius	--	+	--	-

Table 3: **(**Dis)advantages of five methods for determining the mixing index.

Nomenclature

A	Amplitude (-)
d	Diameter (m)
dt	Time step (s)
e	coefficient of restitution (-)
F	Force (kg m s^{-2})
k	spring stiffness (N m^{-1})
m	Mass (kg)
M	Mixing index (-)
N	Number of particles (-)
R	Radius (m)
r_{ij}	Distance between two particles (m)
r_p	particle radius
$\vec{r}$	Particle position (m)
S^2	Variance (-)
$\overline{S}_p$	Sink term (kg m^2 s^{-1})
t	Time (s)
u	Gas velocity (m s^{-1})
V	Volume (m^3)
z	Height (m)
X	System width (m)
Y	System depth (m)
Z	System height (m)

Greek letters

β	Momentum transfer coefficient (kg s^{-1} m^{-2})
ε	Porosity (-)
ϕ	Particle concentration (-)
γ	Damping coefficient (s^{-1})
μ	friction coefficient (-)
ρ	Density (kg m^{-3})
$\overline{\overline{\tau}}_g$	Gas phase stress tensor (kg m^2 s^{-1})
ω	Period (rad s^{-1})

Subscripts

diff	different
fit	fitted
i,j,k,m	particle numbers
M	mean
mf	minimum fluidization
n	normal
sup	superficial
t	tangential

References

Asmar, B.N., Langston, P.A., & Matchett, A.J. A generalised mixing index in distinct element method simulation of vibrated particulate beds. Granular Matter, V4(3), 129-138(2002).

Bokkers, G.A., van Sint Annaland, M., & Kuipers, J.A.M. Mixing and segregation in a bidisperse gas-solid fluidised bed: A numerical and experimental study. Powder Technology, 140(3), 176-186(2004).

Ergun, S. Fluid flow through packed columns. Chemical Engineering Progress, 48, 89-94(1952).

Finnie, G.J., Kruyt, N.P., Ye, M., Zeilstra, C., & Kuipers, J.A.M. Longitudinal and transverse mixing in rotary kilns: A discrete element method approach. Chemical Engineering Science, 60(15), 4083-4091(2005).

Godlieb, W., Deen, N.G., & Kuipers, J.A.M. (2007a). A discrete particle simulation study of solids mixing in a pressurized fluidized bed. In The 12th International Conference on Fluidization, Vancouver - Canada.

Godlieb, W., Deen, N.G., & Kuipers, J.A.M. (2006). Discrete particle simulations of high pressure fluidization. In CHISA 17th International Congress Of Chemical And Process Engineering, Prague - Czech Republic.

Godlieb, W., Deen, N.G., & Kuipers, J.A.M. On the relationship between operating pressure and granular temperature: A discrete particle simulation study. Powder Technology, Submitted, (2007b).

Hoomans, B.P.B., Kuipers, J.A.M., Briels, W.J., & van Swaaij, W.P.M. Discrete particle simulation of bubble and slug formation in a two-dimensional gas-fluidised bed: A hard-sphere approach. Chemical Engineering Science, 51(1), 99-118(1996).

Hoomans, B.P.B., Kuipers, J.A.M., & van Swaaij, W.P.M. Granular dynamics simulation of segregation phenomena in bubbling gas-fluidised beds. Powder Technology, 109(1-3), 41-48(2000).

Kharaz, A.H., Gorham, D.A., & Salman, A.D. Accurate measurement of particle impact parameters. Measurement Science and Technology, 10(1), 31(1999).

Koch, D.L. & Hill, R.J. Inertial effects in suspension and porous-media flows. Annual Review of Fluid Mechanics, 33(1), 619-647(2001).

Lacey, P.C.M. Developments in theory of particulate mixing. J. Apll. Chem., 4, 257(1954).

Link, J.M., Cuypers, L.A., Deen, N.G., & Kuipers, J.A.M. Flow regimes in a spout-fluid bed: A combined experimental and simulation study. Chemical Engineering Science, 60(13), 3425-3442(2005).

Lu, L.-S. & Hsiau, S.-S. Mixing in vibrated granular beds with the effect of electrostatic force. Powder Technology, 160(3), 170-179(2005).

McCarthy, J.J., Khakhar, D.V., & Ottino, J.M. Computational studies of granular mixing. Powder Technology, 109(1-3), 72-82(2000).

Mostoufi, N. & Chaouki, J. Local solid mixing in gas-solid fluidized beds. Powder Technology, 114(1-3), 23-31(2001).

Rhodes, M.J., Wang, X.S., Nguyen, M., Stewart, P., & Liffman, K. Study of mixing in gas-fluidized beds using a dem model. Chemical Engineering Science, 56(8), 2859-2866(2001).

Schutyser, M.A.I., Padding, J.T., Weber, F.J., Briels, W.J., Rinzema, A., & Boom, R. Discrete particle simulations predicting mixing behavior of solid substrate particles in a rotating drum fermenter. Biotechnology and Bioengineering, 75(6), 666-675(2001).

van der Hoef, M.A., Ye, M., van Sint Annaland, M., Andrews, A.T., Sundaresan, S., Kuipers, J.A.M., & Guy, B.M. (2006). Multiscale modeling of gas-fluidized beds, Advances in chemical engineering, vol. Volume 31 (p. 65-149): Academic Press.

Van Puyvelde, D.R. Comparison of discrete elemental modelling to experimental data regarding mixing of solids in the transverse direction of a rotating kiln. Chemical Engineering Science, 61(13), 4462-4465(2006).

Wen, Y.C. & Yu, Y.H. Mechanics of fluidization. Chemical Engineering Progress Symposium, 62, 100-111(1966).

Ye, M., van der Hoef, M.A., & Kuipers, J.A.M. The effects of particle and gas properties on the fluidization of geldart a particles. Chemical Engineering Science, 60(16), 4567-4580(2005).